Performance Analysis of Cooperative NOMA with Dynamic Decode-and-Forward Relaying

Yong Zhou*, Vincent W.S. Wong*, and Robert Schober†
*Department of Electrical and Computer Engineering, The University of British Columbia, Vancouver, Canada
†Institute for Digital Communications, Friedrich-Alexander-University, Erlangen, Germany
E-mail: *{zhou, vincentw}@ece.ubc.ca, †robert.schober@fau.de

***Abstract*—Non-orthogonal multiple access (NOMA) is a promising multiple access technique, which exploits the power domain to enhance the spectral efficiency of the fifth generation (5G) wireless networks. In this paper, we propose a dynamic decode-and-forward (DDF) based cooperative NOMA scheme for downlink transmission to enhance the reception reliability of spatially random users. In DDF-based cooperative NOMA, the user closer to the base station decodes the superimposed mixture of the users' signals received from the base station based on partial reception, and then forwards the signal intended for the far user. To avoid the need for instantaneous channel state information at the base station, we consider random user pairing, where the users are randomly paired for NOMA transmission. Tools from point process theory are utilized to derive the outage probability of the proposed DDF-based cooperative NOMA scheme. Simulation results validate the performance analysis and demonstrate the performance gains of the proposed DDF-based cooperative NOMA scheme over conventional NOMA and cooperative NOMA.**

I. Introduction

Non-orthogonal multiple access (NOMA), as a spectrally-efficient multiple access technique, has the potential to meet the rapidly increasing traffic demands and to support the massive connectivity for billions of devices in the fifth generation (5G) wireless networks [1]. With NOMA, multiple users can be simultaneously served by the same base station using the same frequency channel and spreading code by allocating different transmit powers to the users and applying successive interference cancellation (SIC) at the receiver side.

NOMA has recently attracted significant research interest [2]–[4]. The authors in [2] evaluate the system level performance of downlink NOMA transmission, demonstrating the importance of transmit power allocation and user pairing for the design of efficient NOMA systems. The author in [3] proposes an optimal power allocation approach to maximize the sum rate in multiple-input multiple-output NOMA systems. The impact of user pairing on the outage probability and the sum rate is investigated in [4], where both fixed and cognitive radio-based power allocation are considered. However, in the aforementioned studies, by sharing the frequency channel and transmit power with the near user[1], the performance of the far user can be degraded due to NOMA [5].

Cooperative NOMA can further enhance spectral efficiency by introducing a cooperative diversity gain [6]. A dedicated decode-and-forward (DF) relay is coordinated by the base station to enhance the reception reliability of cell edge users in [7]. The impact of relay selection on the performance of downlink NOMA transmission is investigated in [8]. However, the cooperative NOMA schemes considered in the aforementioned studies require an additional time slot for relay transmission. To address this issue, the authors in [9], [10] analyze the outage probability of full-duplex cooperative NOMA for a two-user scenario, where a near user acts as a full-duplex relay to assist the transmission of a far user. However, full-duplex relaying suffers from a higher hardware implementation complexity compared to half-duplex relaying, and introduces self-interference that can degrade the performance of the near user.

Dynamic decode-and-forward (DDF) relaying [11] is a physical layer cooperation strategy, which allows a half-duplex relay to provide a cooperative diversity gain without the need for additional time slots. The authors in [12] propose a low complexity DDF relaying scheme based on lattice coding/decoding schemes. The authors in [13] characterize the diversity-multiplexing tradeoff for DDF relaying. However, the application of DDF relaying in NOMA systems with spatially random users has not yet been studied.

In this paper, we propose a DDF-based cooperative NOMA scheme for downlink transmission. Specifically, the base station superimposes the signals of two paired NOMA users by allocating different transmit powers to them. The near user decodes both signals based on partial reception, where the reception duration depends on the instantaneous channel gain with respect to the base station. Then, the near user acts as a relay and helps forward the signal intended for the far user. To model the random user locations, the spatial locations of the users are modeled as a homogeneous Poisson point process (PPP). For this network scenario, we analyze the performance of DDF-based cooperative NOMA with *random user pairing*, where the near and the far users are randomly selected for NOMA transmission based on one-bit feedback. The main contributions of this paper are summarized as follows:

- We develop a tractable performance analysis framework for the proposed DDF-based cooperative NOMA scheme for downlink transmission with spatially random users.
- Tools from point process theory are utilized to derive the outage probabilities of the near and the far users for DDF-based cooperative NOMA with random user pairing.
- Simulation results validate the performance analysis. The

[1]For two paired NOMA users, we refer to the user closer to the base station as the near user and to the other user as the far user.

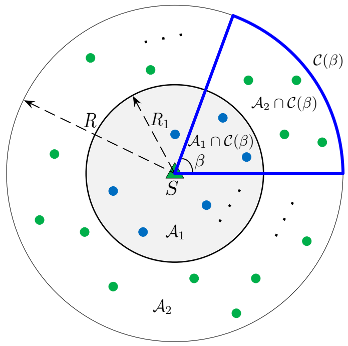

Fig. 1: The network topology for downlink NOMA transmission with spatially random users. The network coverage area is divided into multiple sectors. We focus on a typical sector $\mathcal{C}(\beta)$, where β denotes the angle of the sector. Base station S pairs one user inside $\mathcal{A}_1 \cap \mathcal{C}(\beta)$ and one user inside $\mathcal{A}_2 \cap \mathcal{C}(\beta)$, where $\mathcal{A}_1$ and $\mathcal{A}_2$ are the inner circle and the outer annulus, respectively. The blue and green dots represent the near and the far users, respectively.

proposed DDF-based cooperative NOMA scheme significantly reduces the outage probability of the far user, when compared to conventional NOMA and cooperative NOMA.

The remainder of this paper is organized as follows. Section II describes the network topology and the signal reception model of the proposed DDF-based cooperative NOMA scheme. We characterize the outage probability for random user pairing in Section III. Numerical results are provided in Section IV. Finally, Section V concludes this paper.

II. System Model

A. Network Topology

Consider a downlink transmission scenario, which consists of one base station and multiple users, as shown in Fig. 1. Base station S is located at the center of a circular network coverage area with radius R and is equipped with M antennas. The spatial locations of the users are assumed to follow a homogeneous PPP, denoted as Φ, with density λ, which represents the average number of users per unit area. Each user has a single antenna. The base station and all users operate in the half-duplex mode. The channel between any two transceivers suffers from path loss and quasi-static Rayleigh fading. The fading coefficients are assumed to remain invariant during the transmission of one packet and vary independently across different links, as in [4], [6], [7].

To mitigate co-channel interference and reduce the system complexity, we adopt hybrid medium access and pair two users with NOMA as in [7]–[10]. The network coverage area is evenly divided into M sectors and each sector is served by one antenna of the base station using an orthogonal channel. On the other hand, the users inside the same sector are served using cooperative NOMA. This network architecture facilitates the cooperation of the paired NOMA users, as the near user geographically located between the base station and the far user is more likely to achieve a high cooperation gain [14]. Without instantaneous channel state information (CSI) at the base station, the paired NOMA users can be ordered based on their distances to the base station. It has been shown in [4] that a higher performance gain can be achieved when NOMA users with more diverse channel conditions are paired. In light of this insight, we assume that the network coverage area is divided into two regions, i.e., an inner circle with radius $R_1 < R$ and an outer annulus, denoted by $\mathcal{A}_1$ and $\mathcal{A}_2$, respectively.

As the users within each sector follow the same spatial distribution, we focus on a typical sector, denoted as $\mathcal{C}(\beta)$, where $\beta = 2\pi/M$ is the angle of the sector. We consider random user pairing, where one user inside $\mathcal{A}_1 \cap \mathcal{C}(\beta)$ and one user inside $\mathcal{A}_2 \cap \mathcal{C}(\beta)$ are randomly selected for NOMA transmission.

B. Signal Reception Model

The time is slotted into constant intervals. Within one time slot, the base station's codewords span K blocks of length T symbols each, where T depends on the length of codewords. The cooperative transmission involves two phases. In the first phase, the near user operates in the listening mode and receives the superimposed mixture of the users' signals transmitted by the base station. At a certain time instant, referred to as the *decision time*, the near user successfully decodes the signals intended for the far and the near users based on the NOMA decoding strategy. In the second phase, from the decision time to the end of the time slot, the near user switches to the transmit mode and acts as a relay to help the far user decode its own signal. The decision time is a random variable, which depends on the instantaneous channel condition between the near user and the base station. Without loss of generality, the decision time is assumed to coincide with the end of a block and is denoted as $\mathcal{D}$, which takes on values in the set $\{1, 2, \ldots, K\}$. Specifically, $1 \le \mathcal{D} < K$ corresponds to the case where the near user assists the far user during the last $K - \mathcal{D}$ blocks, while $\mathcal{D} = K$ corresponds to the case that the near user remains silent during the entire time slot.

We denote the paired NOMA users inside sector $\mathcal{C}(\beta)$ as $u_{\rm f}$ and $u_{\rm n}$, which denote the far and near user, respectively. When NOMA is performed to serve users $u_{\rm f}$ and $u_{\rm n}$, the i-th symbol transmitted by base station S is $\alpha_{\rm f}\sqrt{P_S}s_{{\rm f},i} + \alpha_{\rm n}\sqrt{P_S}s_{{\rm n},i}$, where $i = 1, 2, \ldots, KT$, $\alpha_{\rm f}$ and $\alpha_{\rm n}$ denote the power allocation coefficients for users $u_{\rm f}$ and $u_{\rm n}$, respectively, with $\alpha_{\rm f}^2 + \alpha_{\rm n}^2 = 1$, P_S denotes the transmit power of base station S, and $s_{{\rm f},i}$ and $s_{{\rm n},i}$ denote the i-th symbols transmitted to users $u_{\rm f}$ and $u_{\rm n}$, respectively, with $\mathbb{E}\left(|s_{\nu,i}|^2\right) = 1, \nu \in \{{\rm f}, {\rm n}\}$.

In the first phase of transmission, the signal received at user u_ν, $\nu \in \{{\rm f}, {\rm n}\}$, can be expressed as

$$y_{\nu,i} = \left(\alpha_{\rm f}\sqrt{P_S}s_{{\rm f},i} + \alpha_{\rm n}\sqrt{P_S}s_{{\rm n},i}\right) h_\nu \sqrt{\ell(x_\nu)} + z_{\nu,i}, \quad (1)$$

where $i = 1, 2, \ldots, \mathcal{D}T$, decision time $\mathcal{D} \le K$, h_ν denotes the Rayleigh fading channel coefficient between base station S and user u_ν, and $\{z_{\nu,i}\}$ denotes the additive white Gaussian noise (AWGN) at user u_ν with zero mean and variance σ^2. Hence, $|h_\nu|^2$ is an exponential random variable with unit mean. In addition, $\ell(x_\nu) = r_\nu^{-\eta}$ and r_ν denote the path loss and the Euclidean distance between base station S and user u_ν, respectively, where η denotes the path loss exponent, x_ν

denotes the polar coordinate (r_ν, τ_ν) of the location of user u_ν, and τ_ν denotes the angle of user u_ν with respect to base station S. The paired NOMA users are ordered based on their distances with respect to the base station. As $r_{\rm n} \le r_{\rm f}$, we have $\alpha_{\rm n} \le \alpha_{\rm f}$.

Based on (1), the signal-to-interference-plus-noise ratio (SINR) of signal $\{s_{{\rm f},i}\}$ observed at user $u_{\rm n}$ is given by

$$\Gamma_{\rm f\to n} = \frac{\alpha_{\rm f}^2 P_S |h_{\rm n}|^2 \ell(x_{\rm n})}{\alpha_{\rm n}^2 P_S |h_{\rm n}|^2 \ell(x_{\rm n}) + \sigma^2}. \tag{2}$$

After successfully decoding signal $\{s_{{\rm f},i}\}$, the near user removes signal $\{s_{{\rm f},i}\}$ from the received signal $\{y_{{\rm n},i}\}$ by applying SIC, and decodes signal $\{s_{{\rm n},i}\}$ based on the signal-to-noise ratio (SNR) given by

$$\Gamma_{\rm n} = \frac{\alpha_{\rm n}^2 P_S |h_{\rm n}|^2 \ell(x_{\rm n})}{\sigma^2}. \tag{3}$$

On the other hand, by treating signal $\{s_{{\rm n},i}\}$ as co-channel interference, the SINR of signal $\{s_{{\rm f},i}\}$ observed at the far user $u_{\rm f}$ in the first phase of transmission can be expressed as

$$\Gamma_{\rm f|n}^{\rm I} = \frac{\alpha_{\rm f}^2 P_S |h_{\rm f}|^2 \ell(x_{\rm f})}{\alpha_{\rm n}^2 P_S |h_{\rm f}|^2 \ell(x_{\rm f}) + \sigma^2}. \tag{4}$$

According to the principle of DDF relaying, the near user switches from the listening mode to the transmit mode once it has successfully decoded both signals received from base station S, which is possible as soon as the mutual information between user $u_{\rm n}$ and base station S exceeds the target data rates of both users. Hence, the decision time is given by

$$\begin{aligned}\mathcal{D} = \min\Bigg\{K, \min\Bigg\{k \;\Bigg|\; \frac{k}{K}\log_2\left(1+\Gamma_{\rm f\to n}\right) \ge R_{\rm f}^{\rm th},\\ \frac{k}{K}\log_2\left(1+\Gamma_{\rm n}\right) \ge R_{\rm n}^{\rm th}, k \in \{1,2,\ldots\}\Bigg\}\Bigg\},\end{aligned} \tag{5}$$

where $R_{\rm f}^{\rm th}$ and $R_{\rm n}^{\rm th}$ denote the target data rates of the far and the near users, respectively.

After successfully decoding signals $\{s_{{\rm f},i}\}$ and $\{s_{{\rm n},i}\}$, the near user can correctly predict the future transmit symbols of the base station (i.e., $s_{{\rm f},i}$ for $\mathcal{D}T+1 \le i \le KT$) since it knows the base station's codebook. Based on this knowledge, the near user transmits the following signal in the second phase:

$$\tilde{s}_{{\rm f},i} = \begin{cases} s_{{\rm f},i+1}^*, & i = \mathcal{D}T+1, \mathcal{D}T+3, \ldots, KT-1, \\ -s_{{\rm f},i-1}^*, & i = \mathcal{D}T+2, \mathcal{D}T+4, \ldots, KT, \end{cases} \tag{6}$$

where $(\cdot)^*$ denotes complex conjugate.

Base station S is unaware of the mode change at the near user and keeps transmitting the superimposed signals in the second phase. Hence, the signal received at the far user within blocks $[\mathcal{D}T+1, KT]$ reduces to an Alamouti constellation [15] and can be expressed as

$$y_{{\rm f},i} = \begin{cases} \left(\alpha_{\rm f}\sqrt{P_S}s_{{\rm f},i} + \alpha_{\rm n}\sqrt{P_S}s_{{\rm n},i}\right) h_{\rm f}\sqrt{\ell(x_{\rm f})} \\ \quad + \sqrt{P_U}s_{{\rm f},i+1}^* h_{\rm f,n}\sqrt{\ell(x_{\rm f}-x_{\rm n})} + z_{{\rm f},i}, \\ \quad i = \mathcal{D}T+1, \mathcal{D}T+3, \ldots, KT-1, \\ \left(\alpha_{\rm f}\sqrt{P_S}s_{{\rm f},i} + \alpha_{\rm n}\sqrt{P_S}s_{{\rm n},i}\right) h_{\rm f}\sqrt{\ell(x_{\rm f})} \\ \quad - \sqrt{P_U}s_{{\rm f},i-1}^* h_{\rm f,n}\sqrt{\ell(x_{\rm f}-x_{\rm n})} + z_{{\rm f},i}, \\ \quad i = \mathcal{D}T+2, \mathcal{D}T+4, \ldots, KT, \end{cases} \tag{7}$$

where P_U is the transmit power of the near user, and $h_{\rm f,n}$ and $\ell(x_{\rm f} - x_{\rm n})$ denote the Rayleigh fading channel coefficient and the Euclidean distance between users $u_{\rm f}$ and $u_{\rm n}$, respectively.

Through linear processing of the received signal $\{y_{{\rm f},i}\}$, the far user obtains sufficient statistics for decoding, given by

$$\begin{aligned}\tilde{y}_{{\rm f},i} = \left(\alpha_{\rm f}^2 P_S |h_{\rm f}|^2 \ell(x_{\rm f}) + P_U |h_{\rm f,n}|^2 \ell(x_{\rm f}-x_{\rm n})\right) s_{{\rm f},i} + \tilde{z}_{{\rm f},i},\\ i = \mathcal{D}T+1, \ldots, KT,\end{aligned} \tag{8}$$

where $\tilde{z}_{{\rm f},i}$ is given in (9), shown at the top of the next page.

Based on (8) and (9), the SINR of signal $\{s_{{\rm f},i}\}$ observed at the far user $u_{\rm f}$ in the second phase of transmission can be expressed as

$$\Gamma_{\rm f|n}^{\rm II} = \frac{\alpha_{\rm f}^2 P_S |h_{\rm f}|^2 \ell(x_{\rm f}) + P_U |h_{\rm f,n}|^2 \ell(x_{\rm f}-x_{\rm n})}{\alpha_{\rm n}^2 P_S |h_{\rm f}|^2 \ell(x_{\rm f}) + \sigma^2}. \tag{10}$$

Based on the above signal reception model, the SINRs of signal $\{s_{{\rm f},i}\}$ observed at the far user $u_{\rm f}$ depend on whether the near user is in the listening or in the transmit mode. Hence, the achievable transmission rate at the far user $u_{\rm f}$ during the entire time slot is given by

$$R_{\rm f} = \begin{cases} \frac{\mathcal{D}}{K}\log_2\left(1+\Gamma_{\rm f|n}^{\rm I}\right) + \frac{K-\mathcal{D}}{K}\log_2\left(1+\Gamma_{\rm f|n}^{\rm II}\right), & \text{if } 1 \le \mathcal{D} < K, \\ \log_2\left(1+\Gamma_{\rm f|n}^{\rm I}\right), & \text{if } \mathcal{D} = K, \end{cases}$$

where $\Gamma_{\rm f|n}^{\rm I}$ and $\Gamma_{\rm f|n}^{\rm II}$ are given in (4) and (10), respectively.

III. Random User Pairing

In this section, we consider random user pairing, where base station S randomly pairs one user in $\mathcal{A}_1 \cap \mathcal{C}(\beta)$ and one user in $\mathcal{A}_2 \cap \mathcal{C}(\beta)$ for downlink cooperative NOMA transmission based on one-bit feedback. Specifically, each user feeds back 1 or 0 to base station S to indicate whether it is located in $\mathcal{A}_1 \cap \mathcal{C}(\beta)$ or $\mathcal{A}_2 \cap \mathcal{C}(\beta)$. Under the random user pairing strategy, each user has the same opportunity to be served. When there is either no near or no far user, orthogonal multiple access (OMA) can be employed by the base station to serve the randomly selected far or near user. As the main focus of this paper is the performance analysis of DDF-based cooperative NOMA, we assume that there exist at least one near user and one far user.

A. Outage Probability of Near User

For notational ease, we define $\theta(R_{\rm f}^{\rm th}, k) = 2^{R_{\rm f}^{\rm th}K/k} - 1$. If $\alpha_{\rm f}^2 > \theta(R_{\rm f}^{\rm th}, k)\alpha_{\rm n}^2$, the probability that the near user $u_{\rm n}$ can successfully decode both signals from base station S after being in the listening mode for the first $k \in \{1, \ldots, K\}$ blocks can be expressed as

$$\begin{aligned} D_T(k) &= \mathbb{P}\left(\frac{k}{K}\log_2(1+\Gamma_{\rm f\to n}) \ge R_{\rm f}^{\rm th}, \frac{k}{K}\log_2(1+\Gamma_{\rm n}) \ge R_{\rm n}^{\rm th}\right) \\ &\overset{(a)}{=} \mathbb{P}\left(|h_{\rm n}|^2 \ge \left\{\frac{\theta(R_{\rm f}^{\rm th},k)\sigma^2}{(\alpha_{\rm f}^2 - \theta(R_{\rm f}^{\rm th},k)\alpha_{\rm n}^2)P_S\ell(x_{\rm n})}, \frac{\theta(R_{\rm n}^{\rm th},k)\sigma^2}{\alpha_{\rm n}^2 P_S \ell(x_{\rm n})}\right\}\right) \\ &\overset{(b)}{=} \mathbb{E}_{x_{\rm n}}\left[\exp\left(-G(k) r_{\rm n}^\eta\right)\right], \end{aligned} \tag{11}$$

$$\tilde{z}_{\mathrm{f},i}=\begin{cases}\alpha_{\mathrm{n}}\sqrt{P_SP_U\ell(x_{\mathrm{f}})\ell(x_{\mathrm{f}}-x_{\mathrm{n}})}h_{\mathrm{f}}^*h_{\mathrm{f,n}}s_{\mathrm{n},i}^*+\alpha_{\mathrm{f}}\alpha_{\mathrm{n}}P_S\ell(x_{\mathrm{f}})|h_{\mathrm{f}}|^2s_{\mathrm{n},i+1}\\ \quad+\sqrt{P_U\ell(x_{\mathrm{f}}-x_{\mathrm{n}})}h_{\mathrm{f,n}}z_{\mathrm{f},i}^*+\alpha_{\mathrm{f}}\sqrt{P_S\ell(x_{\mathrm{f}})}h_{\mathrm{f}}^*z_{\mathrm{f},i+1},\quad i=\mathcal{D}T+1,\mathcal{D}T+3,\ldots,KT-1,\\ \alpha_{\mathrm{f}}\alpha_{\mathrm{n}}P_S\ell(x_{\mathrm{f}})h_{\mathrm{f}}^2s_{\mathrm{n},i}-\alpha_{\mathrm{n}}\sqrt{P_SP_U\ell(x_{\mathrm{f}})\ell(x_{\mathrm{f}}-x_{\mathrm{n}})}h_{\mathrm{f}}^*h_{\mathrm{f,n}}s_{\mathrm{n},i-1}^*\\ \quad+\alpha_{\mathrm{f}}\sqrt{P_S\ell(x_{\mathrm{f}})}h_{\mathrm{f}}^*z_{\mathrm{f},i}-\sqrt{P_U\ell(x_{\mathrm{f}}-x_{\mathrm{n}})}h_{\mathrm{f,n}}z_{\mathrm{f},i-1}^*,\quad i=\mathcal{D}T+2,\mathcal{D}T+4,\ldots,KT.\end{cases}\tag{9}$$

where (a) follows by substituting (2) and (3), (b) follows from the exponential distribution of channel gain $|h_{\mathrm{n}}|^2$, $\mathbb{E}_{x_{\mathrm{n}}}$ denotes the expectation over the location distribution of user u_{n}, and

$$G(k)=\max\left\{\frac{\theta(R_{\mathrm{f}}^{\mathrm{th}},k)}{\alpha_{\mathrm{f}}^2-\theta(R_{\mathrm{f}}^{\mathrm{th}},k)\alpha_{\mathrm{n}}^2},\frac{\theta(R_{\mathrm{n}}^{\mathrm{th}},k)}{\alpha_{\mathrm{n}}^2}\right\}\frac{\sigma^2}{P_S}.\tag{12}$$

On the other hand, if $\alpha_{\mathrm{f}}^2\le\theta(R_{\mathrm{f}}^{\mathrm{th}},k)\alpha_{\mathrm{n}}^2$, we have $G(k)=\infty$ and $D_T(k)=0$.

Due to random user pairing, the probability density functions (PDFs) of distance r_{n} and angle τ_{n} of user u_{n} with respect to base station S are given by $f_{r_{\mathrm{n}}}(r)=2r/R_1^2$ and $f_{\tau_{\mathrm{n}}}(\tau)=1/\beta$, respectively. If $\alpha_{\mathrm{f}}^2>\theta(R_{\mathrm{f}}^{\mathrm{th}},k)\alpha_{\mathrm{n}}^2$, we have

$$\begin{aligned}D_T(k)&=\int_0^{\beta}\int_0^{R_1}\exp\left(-G(k)r_{\mathrm{n}}^{\eta}\right)\frac{2r_{\mathrm{n}}}{R_1^2}\mathrm{d}r_{\mathrm{n}}\frac{1}{\beta}\mathrm{d}\tau_{\mathrm{n}}\\&=\frac{2}{R_1^2\eta}\left(G(k)\right)^{-2/\eta}\gamma\left(\frac{2}{\eta},G(k)R_1^{\eta}\right),\end{aligned}\tag{13}$$

where $\gamma(a,b)=\int_0^b\exp(-c)c^{a-1}\mathrm{d}c$ is the lower incomplete Gamma function [16].

An outage event occurs at the near user u_{n} when it fails to decode signal $\{s_{\mathrm{n},i}\}$ from base station S after being in the listening mode for all K blocks. The outage probability is the complement of the probability of successful signal reception, which is the probability that near user u_{n} can successfully decode both signals $\{s_{\mathrm{f},i}\}$ and $\{s_{\mathrm{n},i}\}$ from base station S within the entire time slot. Hence, the outage probability of the near user of the DDF-based cooperative NOMA scheme with random user pairing can be expressed as

$$\begin{aligned}q_{\mathrm{out,n}}&=1-D_T(K)\\&\overset{(a)}{=}1-\frac{2}{R_1^2\eta}\left(G(K)\right)^{-2/\eta}\gamma\left(\frac{2}{\eta},G(K)R_1^{\eta}\right),\end{aligned}\tag{14}$$

where (a) follows by setting $k=K$ in (13).

B. Outage Probability of Far User

An outage event occurs at the far user u_{f} when it fails to decode signal $\{s_{\mathrm{f},i}\}$ within the entire time slot. This outage event can be divided into the following two cases: 1) The near user u_{n} fails to decode signals $\{s_{\mathrm{f},i}\}$ and $\{s_{\mathrm{n},i}\}$ after being in the listening mode for the first $K-1$ blocks, and the far user u_{f} also fails to decode signal $\{s_{\mathrm{f},i}\}$ from the base station; 2) The near user u_{n} successfully decodes signals $\{s_{\mathrm{f},i}\}$ and $\{s_{\mathrm{n},i}\}$ after being in the listening mode for the first $\mathcal{D}<K$ blocks, but the far user u_{f} fails to decode signal $\{s_{\mathrm{f},i}\}$ from both the base station and the near user. Hence, the outage probability of the far user for DDF-based cooperative NOMA with random user pairing is given by

$$\begin{aligned}q_{\mathrm{out,f}}=&\,\mathbb{P}\left(\mathcal{D}=K,\log_2\left(1+\Gamma_{\mathrm{f|n}}^{\mathrm{I}}\right)<R_{\mathrm{f}}^{\mathrm{th}}\right)\\&+\mathbb{E}_{x_{\mathrm{n}},x_{\mathrm{f}}}\left(\sum_{k=1}^{K-1}Q_n\left(r_{\mathrm{n}},k\right)Q(k)\right),\end{aligned}\tag{15}$$

where $\mathbb{E}_{x_{\mathrm{n}},x_{\mathrm{f}}}$ denotes the expectation over the location distributions of users u_{n} and u_{f}, and

$$\begin{aligned}Q_n\left(r_{\mathrm{n}},k\right)&=\exp\left(-G(k)r_{\mathrm{n}}^{\eta}\right)-\exp\left(-G(k-1)r_{\mathrm{n}}^{\eta}\right),\\Q(k)&=\mathbb{P}\left(\frac{k}{K}\log_2\left(1+\Gamma_{\mathrm{f|n}}^{\mathrm{I}}\right)+\frac{K-k}{K}\log_2\left(1+\Gamma_{\mathrm{f|n}}^{\mathrm{II}}\right)<R_{\mathrm{f}}^{\mathrm{th}}\right).\end{aligned}\tag{16}$$

Here, $Q_n(r_{\mathrm{n}},k)$ represents the probability that decision time $\mathcal{D}$ is equal to k when the distance between the near user u_{n} and base station S is r_{n}.

Proposition 1. *Assuming the existence of at least one near user and one far user, the outage probability of the far user of the DDF-based cooperative NOMA scheme with random user pairing can be approximated as*

$$\begin{aligned}q_{\mathrm{out,f}}\approx&\,C_1\left(1-\frac{2C_2^{-2/\eta}}{\eta(R^2-R_1^2)}\left(\gamma\left(\frac{2}{\eta},C_2R^{\eta}\right)-\gamma\left(\frac{2}{\eta},C_2R_1^{\eta}\right)\right)\right)\\&+\frac{\pi^3}{(R+R_1)R_1\beta CLJ}\sum_{c=1}^{C}\sqrt{1-\omega_c^2}\sum_{k=1}^{K-1}Q_n(r_{\mathrm{n},c},k)\sum_{l=1}^{L}\sqrt{1-\zeta_l^2}\\&\times\sum_{j=1}^{J}\sqrt{1-\psi_j^2}Q_z(r_{\mathrm{f},j},r_{\mathrm{n},c},\tau_{D,l},k)r_{\mathrm{f},j}^{\eta+1}(\beta-\tau_{D,l})r_{\mathrm{n},c},\end{aligned}\tag{17}$$

if $\alpha_{\mathrm{f}}^2>\theta\left(R_{\mathrm{f}}^{\mathrm{th}},K\right)\alpha_{\mathrm{n}}^2$, *otherwise* $q_{\mathrm{out,f}}=1$, *where* $C_1=1-D_T(K-1)$, $D_T(K-1)$ *and* $Q_n(r_{\mathrm{n},c},k)$ *are given by (11) and (16), respectively,* $C_2=\frac{\theta(R_{\mathrm{f}}^{\mathrm{th}},K)\sigma^2}{(\alpha_{\mathrm{f}}^2-\theta(R_{\mathrm{f}}^{\mathrm{th}},K)\alpha_{\mathrm{n}}^2)P_S}$, $\omega_c=\cos\left(\frac{2c-1}{2C}\pi\right)$, $r_{\mathrm{n},c}=\frac{R_1}{2}(\omega_c+1)$, $\zeta_l=\cos\left(\frac{2l-1}{2L}\pi\right)$, $\tau_{D,l}=\frac{\beta}{2}(\zeta_l+1)$, $\psi_j=\cos\left(\frac{2j-1}{2J}\pi\right)$, $r_{\mathrm{f},j}=\frac{R-R_1}{2}\psi_j+\frac{R+R_1}{2}$, $\phi_i=\cos\left(\frac{2i-1}{2I}\pi\right)$, $z_i=\frac{kR_{\mathrm{f}}^{\mathrm{th}}}{2K}(\phi_i+1)$,

$$\begin{aligned}&Q_z(r_{\mathrm{f}},r_{\mathrm{n}},\tau_D,k)\approx\\&\frac{kR_{\mathrm{f}}^{\mathrm{th}}\pi}{2KI}\sum_{i=1}^{I}\left(\sqrt{1-\phi_i^2}\exp\left(-G_1(z_i,k)r_{\mathrm{f}}^{\eta}\right)G_2(z_i,k)\right.\\&\left.\times\left(1-\exp\left(-G_3(z_i,k)\left(r_{\mathrm{f}}^2+r_{\mathrm{n}}^2-2r_{\mathrm{f}}r_{\mathrm{n}}\cos\tau_D\right)^{\frac{\eta}{2}}\right)\right)\right),\end{aligned}\tag{18}$$

$$G_1(z,k)=\frac{\sigma^2\theta(z,k)}{\left(\alpha_{\mathrm{f}}^2-\theta(z,k)\alpha_{\mathrm{n}}^2\right)P_S},\tag{19}$$

$$G_2(z,k)=\frac{\alpha_{\mathrm{f}}^2\sigma^2\left(\theta(z,k)+1\right)K\ln 2}{\left(\alpha_{\mathrm{f}}^2-\theta(z,k)\alpha_{\mathrm{n}}^2\right)^2P_Sk},\tag{20}$$

$$G_3(z,k)=\frac{\sigma^2\alpha_{\mathrm{f}}^2\left(\theta\left(R_{\mathrm{f}}^{\mathrm{th}}-z,K-k\right)-\theta\left(z,k\right)\right)}{\left(\alpha_{\mathrm{f}}^2-\theta(z,k)\alpha_{\mathrm{n}}^2\right)P_U},\tag{21}$$

and C, I, J, and L are parameters that balance the tradeoff between the computational complexity and the accuracy of the approximation.

Proof. Please refer to the Appendix. $\square$

The accuracy of the approximations in Proposition 1 is verified in Section IV by computer simulations. According to Proposition 1, the outage probability of the far user for DDF-based cooperative NOMA with random user pairing depends on the spatial distribution of the users, the transmit power allocation coefficients, and the target data rates of both users.

IV. Performance Evaluation

In this section, we present simulation and analytical results for the proposed DDF-based cooperative NOMA scheme, and compare them with corresponding results for conventional NOMA [4] and cooperative NOMA [6]. To facilitate cooperative NOMA in one time slot, the base station transmits to the near and the far users in the first half of the time slot using NOMA, and the near user acts as a relay in the second half of the time slot if it can successfully decode the signal intended for the far user. Hence, the spectral efficiency is reduced by half. At the end of the time slot, the far user decodes its signal using maximum ratio combining. In the simulation, a circular network coverage area with radius $R = 300$ m is considered. The noise power and path loss exponent are set to -60 dBm and 3, respectively. Unless specified otherwise, we set $K = 20$, $\beta = \pi/3$, $\lambda = 0.005\ \mathrm{nodes/m^2}$, $R_1 = 100$ m, and $P_S = P_U$. We assume Rayleigh fading channels. We set $C = I = J = L = 30$, which are sufficiently large values to guarantee the accuracy of the approximation.

Fig. 2 shows the impact of the transmit power on the outage probabilities of the near and the far users for all considered schemes. The simulation results are in good agreement with the analytical (A) results, which validates the performance analysis. When the transmit power is smaller than 20 dBm, the outage probability of the far user of DDF-based cooperative NOMA is higher than that of the near user, as the far user suffers from a larger path loss. By exploiting cooperative diversity, the slope of the outage probability of the far user of DDF-based cooperative NOMA is higher than that of the near user. Hence, when the transmit power is larger than 20 dBm, the outage probability of the far user is lower than that of the near user. The outage probabilities of the near and the far users of DDF-based cooperative NOMA are lower than those of cooperative NOMA, because cooperative NOMA reduces the spectral efficiency by half to achieve cooperative diversity in one time slot. In terms of the outage probability of the far user, DDF-based cooperative NOMA always outperforms conventional NOMA by exploiting cooperative diversity. On the other hand, DDF-based cooperative NOMA and conventional NOMA achieve the same outage probability for the near user. This is because for both schemes an outage event occurs if and only if the near user cannot successfully decode its signal from the base station by the end of the time slot.

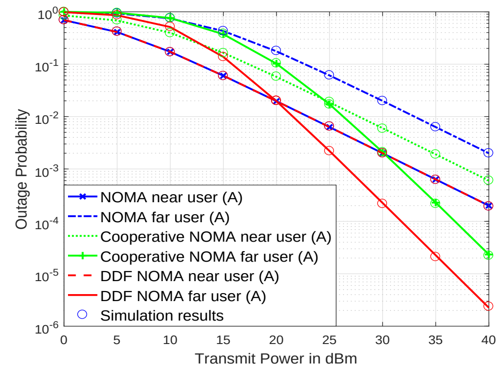

Fig. 2: Outage probability versus transmit power with parameters $R_{\mathrm{f}}^{\mathrm{th}} = R_{\mathrm{n}}^{\mathrm{th}} = 1$ bit per channel use (BPCU), $\alpha_{\mathrm{f}}^2 = 0.8$, and $\alpha_{\mathrm{n}}^2 = 0.2$.

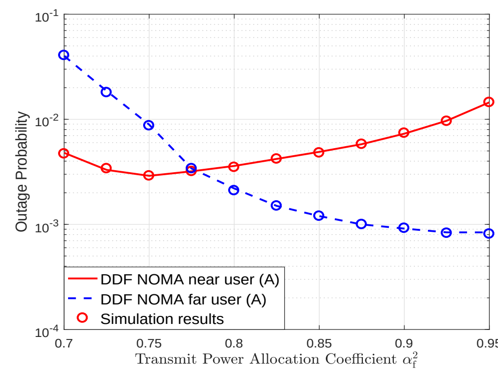

Fig. 3: Outage probability versus transmit power allocation coefficient with parameters $R_{\mathrm{f}}^{\mathrm{th}} = R_{\mathrm{n}}^{\mathrm{th}} = 1.5$ BPCU and $P_S = 30$ dBm.

Fig. 3 illustrates the impact of the transmit power allocation coefficients on the outage probabilities of the near and the far users of DDF-based cooperative NOMA. By increasing α_{f}^2 from 0.7 to 0.75, the outage probability of the near user decreases. This is because increasing α_{f}^2 leads to a higher probability of successfully performing SIC at the near user according to (2). By further increasing α_{f}^2 from 0.75 to 0.95, the outage probability of the near user increases. This is because the benefits introduced by increasing the probability of successful SIC cannot compensate for the reduction in the SNR of the signal intended for the near user. On the other hand, by increasing α_{f}^2, the outage probability of the far user keeps decreasing, as more power is allocated to transmit the signal intended for the far user.

Fig. 4 shows the impact of the choice of the target data rates of the near and the far users on the outage probabilities. When the target data rates are smaller (e.g., $R_{\mathrm{n}}^{\mathrm{th}} = R_{\mathrm{f}}^{\mathrm{th}} = 1$ BPCU), the outage probability of the near and the far users of DDF-based cooperative NOMA are lower, as smaller reception thresholds are required for successful decoding. Moreover, the impact of the target data rates on the outage probability of the far user is larger than that on the outage probability of the near user. In particular, the transmit power required for the far user to achieve a better performance than the near user decreases from 27 dBm to 20 dBm when the target data rates are reduced from $R_{\mathrm{n}}^{\mathrm{th}} = R_{\mathrm{f}}^{\mathrm{th}} = 1.5$ BPCU to $R_{\mathrm{n}}^{\mathrm{th}} = R_{\mathrm{f}}^{\mathrm{th}} = 1$ BPCU.

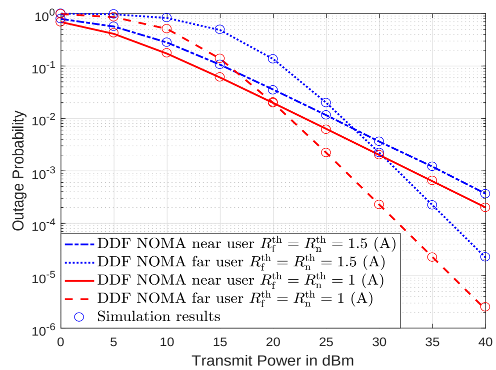

Fig. 4: Outage probability for different target data rates when $\alpha_f^2 = 0.8$ and $\alpha_n^2 = 0.2$.

V. Conclusion

In this paper, we proposed a DDF-based cooperative NOMA scheme for downlink transmission with spatially random users. Based on one-bit feedback, we considered a random user pairing strategy. We characterized the received SINRs observed at the far user when the near user is in the listening and transmit modes, respectively. Based on the SINRs, we derived the outage probabilities of the near and the far users for the proposed scheme using tools from point process theory. Simulation results validated the performance analysis and demonstrated the performance gains of the proposed scheme over conventional NOMA and cooperative NOMA. For future work, we will study the performance of DDF-based cooperative NOMA for alternative user pairing strategies exploiting limited CSI knowledge.

Appendix: Proof of Theorem 1

The probabilities of the first and the second cases are denoted as $q_{\mathrm{out,f}}^{\mathrm{I}}$ and $q_{\mathrm{out,f}}^{\mathrm{II}}$, respectively. The probability for the first case is given by

$$\begin{aligned} q_{\mathrm{out,f}}^{\mathrm{I}} &\overset{(a)}{=} \mathbb{P}(\mathcal{D}=K)\,\mathbb{P}\left(\frac{\alpha_f^2 P_S |h_f|^2 \ell(x_f)}{\alpha_n^2 P_S |h_f|^2 \ell(x_f) + \sigma^2} < \theta(R_f^{\mathrm{th}}, K)\right) \\ &= C_1 \mathbb{E}_{x_f}\left(1 - \exp\left(-C_2 r_f^{\eta}\right)\right), \end{aligned} \tag{22}$$

where $C_1 = 1 - D_T(K-1)$ and (a) follows from the independent channel fading assumption across different links.

Given the existence of the far user and due to the random user pairing, the PDFs of distance r_f and angle τ_f of user u_f with respect to base station S are given by $f_{r_f}(r) = 2r/(R^2 - R_1^2)$ and $f_{\tau_f}(\tau) = 1/\beta$, respectively. We have

$$q_{\mathrm{out,f}}^{\mathrm{I}} = C_1\left(1 - \frac{2C_2^{-2/\eta}}{\eta(R^2 - R_1^2)}\left(\gamma\left(\frac{2}{\eta}, C_2 R^{\eta}\right) - \gamma\left(\frac{2}{\eta}, C_2 R_1^{\eta}\right)\right)\right).$$

The SINRs of signal $\{s_{f,i}\}$ observed at the far user u_f in the first and the second phases are correlated as the value of $|h_f|^2$ does not change throughout the time slot. To facilitate the calculation of the probability for the second case, we denote the achievable transmission rate at the far user u_f in the first phase by $Z = \frac{k}{K}\log_2\left(1 + \Gamma_{f|n}^{\mathrm{I}}\right)$. The PDF of random variable Z can be calculated as

$$f_Z(z) = \exp\left(-G_1(z,k) r_f^{\eta}\right) G_2(z,k) r_f^{\eta}, \tag{23}$$

where $G_1(z,k)$ and $G_2(z,k)$ are defined in (19) and (20), respectively.

For a given decision time k, we have

$$\begin{aligned} Q(k) &= \mathbb{E}_Z\left[\mathbb{P}\left(\frac{K-k}{K}\log_2\left(1 + \Gamma_{f|n}^{\mathrm{II}}\right) < R_f^{\mathrm{th}} - Z \,\middle|\, Z\right)\right] \\ &= \mathbb{E}_Z\left(1 - \exp\left(-\frac{G_3(z,k)}{\ell(x_f - x_n)}\right)\right), \end{aligned} \tag{24}$$

where $G_3(z,k)$ is defined in (21). By substituting (23) into (24), we can obtain $Q(k)$ conditioned on x_n and x_f.

Let $\tau_D = |\tau_f - \tau_n|$ denote the absolute value of the angle difference between τ_f and τ_n. As angles τ_f and τ_n are uniformly distributed within $[0, \beta]$ and independent from each other, we can calculate the PDF of τ_D as

$$f(\tau_D) = (2\beta - 2\tau_D)/\beta^2, \quad \tau_D \in [0, \beta]. \tag{25}$$

By substituting the PDFs of r_n, r_f, τ_D, and Z into (15), we obtain $q_{\mathrm{out,f}}^{\mathrm{II}}$ in the form of multiple integrals. By further applying Gauss-Chebyshev quadrature to approximate the integrals by summations, we obtain (17).

References

[1] V.W.S. Wong, R. Schober, D.W.K. Ng, and L. C. Wang, *Key Technologies for 5G Wireless Systems*. Cambridge University Press, 2017.

[2] A. Benjebbovu, A. Li, Y. Saito, Y. Kishiyama, A. Harada, and T. Nakamura, "System-level performance of downlink NOMA for future LTE enhancements," in *Proc. IEEE Globecom*, Atlanta, GA, Dec. 2013.

[3] J. Choi, "On the power allocation for MIMO-NOMA systems with layered transmissions," *IEEE Trans. Wireless Commun.*, vol. 15, no. 5, pp. 3226–3237, May 2016.

[4] Z. Ding, P. Fan, and H. V. Poor, "Impact of user pairing on 5G non-orthogonal multiple access downlink transmissions," *IEEE Trans. Veh. Technol.*, vol. 65, no. 8, pp. 6010–6023, Aug. 2016.

[5] Y. Zhou and V.W.S. Wong, "Stable throughput region of downlink NOMA transmissions with limited CSI," in *Proc. IEEE ICC*, Paris, France, May 2017.

[6] Z. Ding, M. Peng, and H. V. Poor, "Cooperative non-orthogonal multiple access in 5G systems," *IEEE Commun. Lett.*, vol. 19, no. 8, pp. 1462–1465, Aug. 2015.

[7] J.-B. Kim and I.-H. Lee, "Non-orthogonal multiple access in coordinated direct and relay transmission," *IEEE Commun. Lett.*, vol. 19, no. 11, pp. 2037–2040, Nov. 2015.

[8] Z. Ding, H. Dai, and H. V. Poor, "Relay selection for cooperative NOMA," *IEEE Wireless Commun. Lett.*, vol. 5, no. 4, pp. 416–419, Aug. 2016.

[9] C. Zhong and Z. Zhang, "Non-orthogonal multiple access with cooperative full-duplex relaying," *IEEE Commun. Lett.*, vol. 20, no. 12, pp. 2478–2481, Dec. 2016.

[10] Z. Zhang, Z. Ma, M. Xiao, Z. Ding, and P. Fan, "Full-duplex device-to-device aided cooperative non-orthogonal multiple access," *IEEE Trans. Veh. Technol.*, to appear, 2017.

[11] K. Azarian, H. El Gamal, and P. Schniter, "On the achievable diversity-multiplexing tradeoff in half-duplex cooperative channels," *IEEE Trans. Inf. Theory*, vol. 51, no. 12, pp. 4152–4172, Dec. 2005.

[12] A. Murugan, K. Azarian, and H. El Gamal, "Cooperative lattice coding and decoding in half-duplex channels," *IEEE J. Sel. Areas Commun.*, vol. 25, no. 2, Feb. 2007.

[13] K. R. Kumar and G. Caire, "Coding and decoding for the dynamic decode and forward relay protocol," *IEEE Trans. Inf. Theory*, vol. 55, no. 7, pp. 3186–3205, Jul. 2009.

[14] Y. Zhou and W. Zhuang, "Throughput analysis of cooperative communication in wireless ad hoc networks with frequency reuse," *IEEE Trans. Wireless Commun.*, vol. 14, no. 1, pp. 205–218, Jan. 2015.

[15] S. M. Alamouti, "A simple transmit diversity technique for wireless communications," *IEEE J. Sel. Areas Commun.*, vol. 16, no. 8, pp. 1451–1458, Oct. 1998.

[16] I. S. Gradshteyn and I. M. Ryzhik, *Table of Integrals, Series, and Products*. Academic Press, 2014.